# Inelastic Scattering of Gamma Rays by Bound Electrons

J. VARMA* AND M. A. ESWARAN
*Atomic Energy Establishment Trombay, Bombay, India*
(Received April 12, 1962)

With incident $\gamma$ rays of energy 662 keV the energy spectrum of the photons inelastically scattered by the $K$-shell electrons of lead has been studied, employing NaI(Tl) scintillation spectrometers and coincidence techniques. The energy spectrum of the $\gamma$ rays scattered at 124° to the incident direction is observed to be a continuum from zero energy to about 570 keV. At 60° also the spectrum shows the same trend. The observed photon energy spectrum is found to differ to a very great extent from that calculated on the basis of the various nonrelativistic theories.

The cross section for the inelastic scattering of the 662-keV $\gamma$ rays by a $K$-shell electron of lead, at 124°, for scattered photon energy greater than 160 keV is estimated to be (1.78±0.16) times that by a free electron.

## INTRODUCTION

SINCE the discovery of the Compton effect and its explanation, a large amount of work has been done to study the inelastic scattering of x rays.[1] Theoretical calculations about the energy of the scattered x rays and the cross section for the process, at various angles to the incident photon direction, have been verified. In all the above studies, the electron responsible for the scattering of the photon has been regarded to be free and at rest. DuMond,[2–4] for the first time, demonstrated the effect of the momentum of the electron in the atomic shell, on the energy of the scattered x rays. On scattering the $K$ radiations of Mo from carbon, helium, and hydrogen, it was observed that the Compton line was broadened. From the shape of this line, and applying the laws of conservation of energy and momentum, DuMond calculated the momenta distributions of electrons in the shells of the scattering atoms. It was also shown[5,3] that the wavelength of the x rays scattered by bound electrons is smaller than that expected if the electrons were free, the difference being proportional to the square of the incident wavelength $\lambda$. A semiclassical treatment[6] gives the defect in the Compton shift to be proportional to $B\lambda^2$, where $B$ is the binding energy of the electron in the atomic shell. Bloch[7] has calculated by a nonrelativistic treatment the shift and the shape of the Compton line for the scattering of x rays by electrons loosely bound in atomic shells. No study, theoretical or experimental, has so far been made of the energy spectrum of the inelastically scattered $\gamma$ rays from tightly bound electrons in an atom which would have large momenta and binding energy. Brini *et al.*[8] have found the cross section for the scattering of 662-keV $\gamma$ rays by the $K$-shell electrons of lead to be an order of magnitude larger than that by a free electron. Recent measurements of Motz and Missoni[9] on scattering of 662-keV $\gamma$ rays by the $K$-shell electrons of gold give the cross section for the process as 1.4 times that for free electrons, when the angle of scattering is 110°. The angular dependence of the cross section for small angles is found to be similar to that given by Grodstein's[10] calculations for an electron in the hydrogen atom.

Since the present work was completed, Sujkowski and Nagel[11] have reported the energy spectrum of the 662-keV $\gamma$ rays scattered by the $K$-shell electrons of lead and the cross section for the process. These authors, however, have not taken into consideration the coincidences between the photons Compton-scattered by the electrons, other than those in the $K$ shell, and the x rays emitted when the Compton electrons produce $K$-shell ionization in the scatterer. As discussed later in the text, this effect could make an appreciable contribution to the observed gamma-ray spectrum.

In the measurements presented here, the spectrum of the 662-keV $\gamma$ rays, inelastically scattered by the $K$-shell electrons of lead, has been studied with the help of NaI(Tl) scintillation spectrometers and coincidence techniques. The measurements have been made at the scattering angles of 124° and 60° to the incident direction.

When a photon is scattered incoherently by an electron bound in the $K$ shell of a lead atom, the electron is knocked out of its orbit, leaving a vacancy in the $K$ shell. The vacancy is filled in a very short time ($\approx 10^{-16}$ sec) by transitions from the outer shells and emission of the characteristic $K$ x rays of lead. The experiment consists of studying the spectrum of the scattered $\gamma$ rays, at a certain angle to the incident

* Present address: Physics Department, University of Delhi, Delhi, India.

[1] R. D. Evans, *Encyclopedia of Physics*, edited by S. Flügge (Springer-Verlag, Heidelberg, 1958), Vol. 34, p. 218.
[2] J. W. M. DuMond, Revs. Modern Phys. **5**, 1 (1933).
[3] J. W. M. DuMond and H. A. Kirkpatrick, Phys. Rev. **52**, 419 (1937).
[4] H. A. Kirkpatrick and J. W. M. DuMond, Phys. Rev. **54**, 802 (1938).
[5] P. A. Ross and P. Kirkpatrick, Phys. Rev. **45**, 135 (1934); **46**, 668 (1934).
[6] P. A. Ross and P. Kirkpatrick, Phys. Rev. **45**, 223 (1934).
[7] F. Bloch, Phys. Rev. **46**, 674 (1934).
[8] D. Brini, E. Fuschini, N. T. Grimelini, and D. S. R. Murty, Nuovo cimento **16**, 727 (1960).
[9] J. W. Motz and G. Missoni, Phys. Rev. **124**, 1458 (1961).
[10] G. White Grodstein, National Bureau of Standards Circular No. 583 (U. S. Government Printing Office, Washington, D. C., 1957).
[11] Z. Sujkowski and B. Nagel, Arkiv Fysik **20**, 323 (1961).

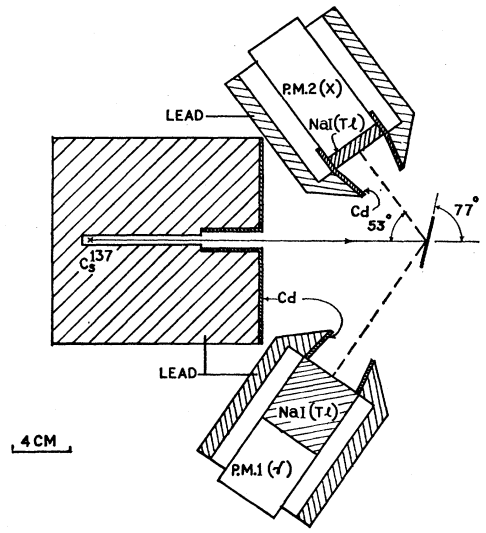


FIG. 1. Experimental arrangement.

beam, in coincidence with the $K$ x rays of lead, thereby eliminating the process taking place in the other shells. The spectrum thus obtained can be compared with the noncoincident $\gamma$ ray from the Compton scattering by electrons in the outer shells of the lead atoms.

## INSTRUMENTATION

The beam of 662-keV $\gamma$ rays was obtained by collimating the radiations from a 40-mCi $Cs^{137}$ source, deposited in a cavity $\frac{1}{4}$ in. diam$\times\frac{1}{4}$ in. deep made in Perspex. The lead collimator, having a diameter of $\frac{1}{4}$ in., was 3 in. long. At the end of this collimator was kept another lead piece 1 in. thick having a hole of $\frac{1}{2}$ in. diam. The front side of this lead piece and the sides of the hole in it, were covered with $\frac{1}{16}$-in. thick Cd sheet to absorb the lead x rays originating in the collimator. Figure 1 shows the geometry of the experiment. The scatterer was a lead foil of size $1\times1\frac{1}{2}$ in. and 0.001, 0.002, or 0.003 in. thick mounted on a thin steel wire frame. The frame size was such as not to intercept the gamma-ray beam. On one side of the scatterer, at an angle of 127° to the incident beam, was placed the x-ray detector. On the other side, the gamma-ray detector was placed on an arm which could be rotated round the axis passing through the center of the scatterer and the gamma-ray beam.

The gamma-ray detector, a 1.75-in. diam$\times$2-in. thick NaI(Tl) crystal mounted on an RCA 6810-A photomultiplier tube, subtended a half-angle of 11° at the center of the scatterer. The x-ray detector was a 1.6-in. diam$\times$0.3-in. thick crystal of NaI(Tl) mounted directly on an RCA 6810-A tube. The casing of the x-ray crystal was such as to absorb a minimum of the x rays. The $K$ x-ray peak in this detector was selected in a 4V wide channel of a single-channel kick-sorter. The channel accepted about half of the total x-ray counts in the peak. The gamma-ray spectrum in the other counter coincident with the x rays, was recorded on a twenty-channel kick-sorter of a modified Gatti[12] type, built in this laboratory. As the block diagram of Fig. 2 shows, the coincidence set up was of the standard fast-slow type, with a fast resolving time $2\tau=0.2$ $\mu$sec. The chance coincidence rate was about 2 to 3% of the real coincidence rate. The phototube boxes containing the voltage divider resistors, inverter, and cathode follower circuits were found to get hot due to about 40 W power dissipated in each of them. Cooling these boxes with fans stabilized the pulse height from the two boxes to better than $\pm2$%. This amount of stabilization was adequate for the experiment, because the width of the scattered gamma-ray peak, due to the large angle of acceptance, was about 16%.

## PROCEDURE

When the channel in the x-ray counter is selecting the energy region of the lead $K$ x-ray peak, and the other detector is accepting the complete energy spectrum of $\gamma$ rays, the various ways in which coincidences could arise are as follows:

(a) Inelastic scattering of $\gamma$ rays in the $K$ shell gives rise to $K$ x rays and scattered $\gamma$ rays. The coincidence rate due to this effect, which is under study here, clearly varies linearly with the thickness $t$ of the scatterer in the path of the beam.

(b) A photoelectron produced in the $K$ shell (thus giving rise to a $K$ x ray) by the incident $\gamma$ rays, may ionize the $K$ shell of a lead atom during the course of slowing down. This would give rise to an x-ray peak in the gamma-ray counter. For scatterer thickness smaller than the range of the photoelectrons, this coincidence rate would vary as $\approx t^2$.

(c) Compton electrons, ejected from outer shells, producing $K$ x rays during slowing down as in (b), would give rise to a peak in the gamma-ray spectrum similar in energy and shape to the singles spectrum.

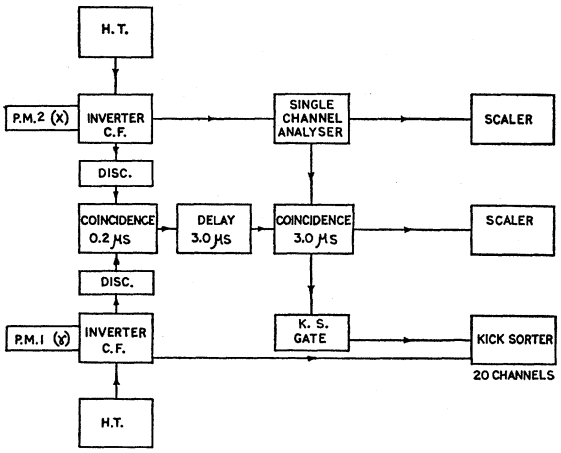


FIG. 2. Block diagram of the electronic apparatus.

[12] E. Gatti, Nuovo cimento **11**, 153 (1954).

For small thickness of the scatterer this effect is also proportional approximately to $t^2$.

(d) Photoelectrons and Compton electrons produce bremsstrahlung in the scatterer. When the low-energy bremsstrahlung is detected in the x-ray channel, this gives rise to an x-ray peak and a Compton gamma-ray peak in the gamma-ray counter. For the x rays from the photoelectric effect being detected in the x-ray channel, this effect would contribute to a continuous gamma-ray spectrum in the gamma-ray counter with a shape like that of the bremsstrahlung spectrum. This effect would also be proportional to $t^2$.

(e) In spite of collimation there is a substantial counting rate in the two detectors due to the $\gamma$ rays scattered by air and those that pass through the lead shields. These $\gamma$ rays could scatter from one crystal to the other to give coincidences. This coincidence rate is constant and independent of the scatterer material.

(f) $\gamma$ rays entering into one of the detectors after scattering from the scatterer, may scatter again (in single or multiple processes) into the other detector, giving coincidences. This coincidence rate is dependent upon the scatterer thickness but not upon its material.

(g) There is background due to cosmic rays and other radioactive sources present in the laboratory. The coincidence rate would be constant in time.

(h) Coincidences arise due to second-order effects—a combination of two or more of the above-mentioned processes. This coincidence rate is expected to be negligible and would be dependent upon $t^2$, or higher powers of $t$.

It would be noted that the coincidence rates due to (e), (f), and (g), which could be termed geometrical background, could be determined in a single experiment in which the coincidence spectrum is recorded by replacing the lead scatterer by one of aluminum. The Al scatterer should contain about the same number of electrons as the lead scatterer. As the cross section[13] for the $K$-shell ionization in heavy elements by a fast electron is of the order of $10^{-22}$ cm$^2$/atom, the effects (b) and (c) contribute to the coincidence spectrum to a considerable extent. However, the contribution to the coincidence spectrum due to the effects (b), (c), and also (d) and (h) could be accounted for if the coincidence spectrum is recorded for various thicknesses of the scatterer. The scatterer thicknesses used in this experiment were 28.6, 58.8, and 93.3 mg/cm$^2$.

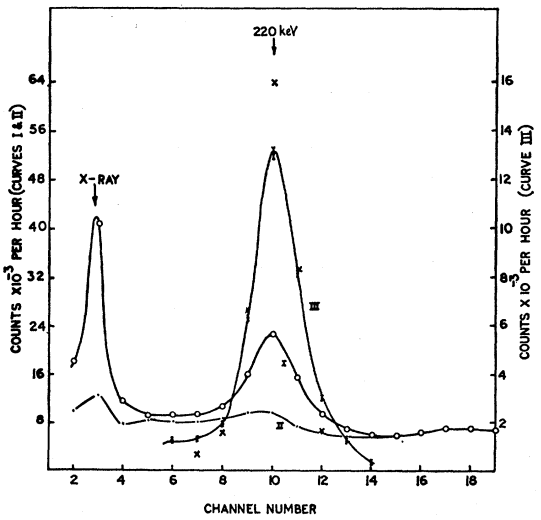


FIG. 3. Pulse-height spectrum due to $\gamma$ rays scattered at 124° to the beam. Curve I was taken with 93.3-mg/cm$^2$-thick lead scatterer and Curve II with only the supporting frame in position. Curve III is the difference of I and II plotted in the peak region only. The crosses give the counts taken with an aluminum scatterer of thickness 72.0 mg/cm$^2$ (background subtracted).

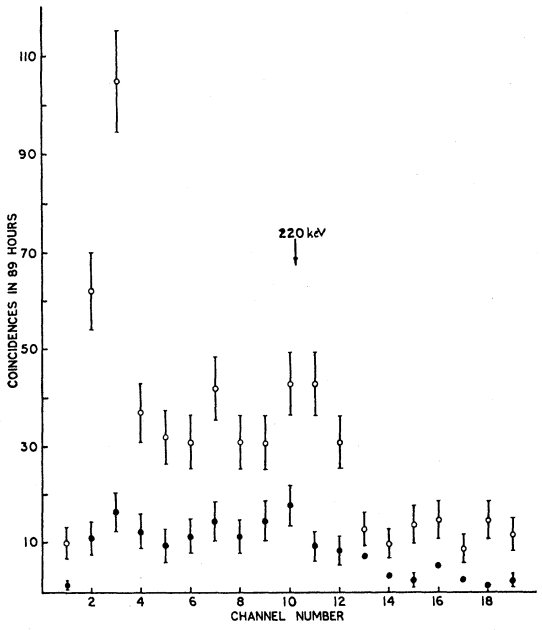


FIG. 4. Pulse-height spectrum due to the $\gamma$ rays scattered at 124° to the beam in coincidence with $K$ x rays of lead. The open circles represent counts with a 28.6-mg/cm$^2$ thick lead scatterer and the closed circles represent the background taken with a 21.3-mg/cm$^2$-thick aluminum scatterer.

When the gamma-ray counter is fixed at 124° to the incident beam and the 93.3-mg/cm$^2$ lead foil used as the scatterer, curve I of Fig. 3 is obtained as the pulse-height spectrum. Curve II is obtained when the lead foil is replaced by the wire frame supporting it. Curve III obtained by subtraction of II from I, is the energy spectrum of the $\gamma$ rays due to the scatterer. The x-ray peak due to the photoelectric effect in the lead scatterer and the Compton-scattered gamma-ray peak are evident. The crosses on curve III represent the spectrum obtained with a 72-mg/cm$^2$ Al foil, and show that this Al foil is suitable for obtaining the geometrical background in this case. After the singles spectrum was recorded, as in Fig. 3, the kick-sorter was switched

[13] H. S. W. Massey and E. H. S. Burhop, *Electronic and Ionic Impact Phenomena* (Oxford University Press, New York, 1952), p. 154.

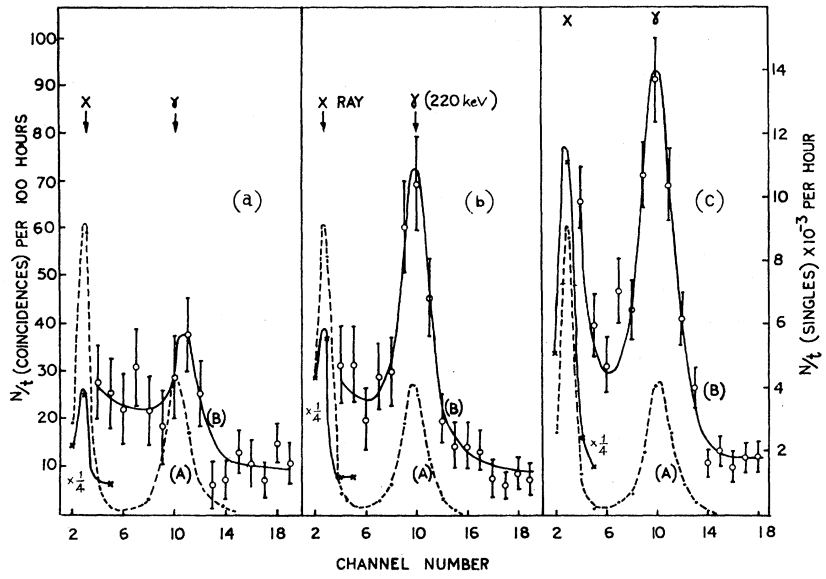


FIG. 5. Pulse-height spectrum due to $\gamma$ rays scattered at 124° to the beam in singles and in coincidence with the $K$ x rays of lead. Figures (a), (b), (c) represent the observations taken for three different lead scatterers of thicknesses 28.6, 58.8, and 93.3 mg/cm², respectively. The dashed curves [shown as (A)] are the singles spectra after normalization for the same thickness (see text). The solid curves [shown as (B)] are the coincidence spectra, also normalized to the same thickness as in the case of singles. Background has been subtracted for each spectrum. The peaks at the x-ray energy and at 220 keV, varying in height approximately as the square of the thickness of the scatterer, caused by the secondary effects, and superimposed on a broad continuous spectrum linearly dependent on the scatterer thickness, can clearly be identified in the figure.

to record the coincidence spectrum for a period of 12 to 16 h with the lead scatterer in position. The whole procedure was repeated every day till enough coincidences were accumulated in each channel. The positions of the peaks in the x ray and the gamma-ray counters were checked every day and corrected for any slight variation. A similar experiment was performed to determine the background by replacing the lead scatterer with an equivalent aluminum scatterer. In Fig. 4 are shown the coincidence spectra from 28.6-mg/cm² lead and 21.3-mg/cm² aluminum scatterers recorded for 89 h each.

Similar experiments were repeated with the other two lead scatterers. It was observed that at this angle the background was almost independent of the thickness of the Al scatterer and was about the same as in Fig. 4. In Fig. 5 (a), (b), and (c) are shown the singles and coincidence spectra obtained for the three thicknesses of the scatterer after subtracting the background, and dividing the counting rate by the thickness of the respective scatterer (the thickness of the thinnest scatterer is taken as unity). By this procedure, the part of the spectrum varying as $t$ remains constant, while the part varying at $t^2$ keeps increasing. The effects (a), (b), and (c) described earlier show up clearly, in the three figures of Fig. 5. A comparison with the singles spectrum shows that the coincidence spectrum is composed partly of x-ray and gamma-ray peaks, due to the secondary effects (b) and (c) mentioned earlier, the intensity of which vary as $\approx t^2$. These peaks are superimposed over a continuous spectrum extending from low energies, to energies higher than that of the normal Compton-scattered $\gamma$ rays. The intensity of this continuum is constant in the three figures (a), (b), and (c) showing it to vary linearly with the scatterer thickness. The correctness of the normalization for the three thicknesses is evident from the identical singles spectra in the three cases.

To study the higher energy part of the continuous spectrum, the gain of the gamma-ray counter was reduced and the coincidence spectrum recorded for the 93.3-mg/cm² lead scatterer. In Fig. 6 are shown the singles and coincidence spectra after subtracting the respective backgrounds. To separate the continuous spectrum due to the primary effect (a) from that due to (c), mentioned earlier, a spectrum similar to that for singles, with an appropriate height, was subtracted from the coincidence spectrum. The resultant dashed curve shows that the spectrum of the $\gamma$ rays inelastically scattered by the $K$-shell electrons of lead extends up to about 600 keV. In Fig. 7 are shown similar observations, obtained with the 58.8-mg/cm² lead scatterer at a scattering angle of 60° to the incident beam. As the Compton electron energy at this angle is only about 260 keV, an experiment similar to that described in Fig. 5 could not be done with the available lead foils. It is to be observed that at this angle also the inelastically scattered gamma-ray spectrum extends up to about 600 keV. An effort was made to study the low-energy part of the spectrum of the $\gamma$ ray scattered at 124°, but due to poor statistics no better information than that from Fig. 5 (a) could be obtained.

From the spectrum of the $\gamma$ rays scattered by the $K$-shell electrons, the cross section for the process can be estimated in terms of the free-electron cross section, knowing the absolute detection efficiency of the x-ray counter for the lead x rays. The spectrum of $\gamma$ rays scattered from the Al scatterer can be regarded as that from free electrons. The detection efficiency of the x-ray detector was determined by a $\beta$-x coincidence experiment using a $Au^{198}$ source. This source emits $\beta$ particles, followed predominantly (98.6%) by 412-keV

$\gamma$ rays, or its conversion electrons and Hg x rays, which are close in energy to the Pb x rays.[14] The $Au^{198}$ source was placed at the position corresponding to the center of the scatterer, without disturbing the x-ray detector. An anthracene counter was used as a $\beta$-ray detector. Care was taken to avoid unwanted coincidences by discriminating against the pulses due to conversion electrons in the $\beta$ counter. After correcting for background counting rates in the two detectors, the efficiency of the x-ray detector was found to be $(8.4\pm0.4)\times10^{-3}$. This agrees very well with the value obtained from the calculations of solid angle, the absorption coefficient of the x ray in NaI(Tl), the iodine x-ray escape correction, the absorption of x rays before reaching the detector, and the fluorescence yield of the x rays in lead. To determine the effect of the size of the scatterer, a point source of $Hg^{203}$ was placed in place of the scatterer. The source was moved over the area of the scatterer and the counting rate in the x-ray peak, in the x-ray counter, was recorded. It was found that the mean value for the extreme positions of the source was within 2% of that when the source was at the center. As the intensity of the gamma-ray beam hitting the scatterer at these extremes was very low, a correction for the finite size of the scatterer was considered unnecessary.

The corrected coincidence spectrum of Fig. 6 (dashed curve) was reconstructed graphically to obtain the energy spectrum of the scattered photons, by taking into account the absorption of $\gamma$ rays in the NaI(Tl) crystal, the areas of the photopeaks and the Compton distributions, and the self-absorption in the scatterer

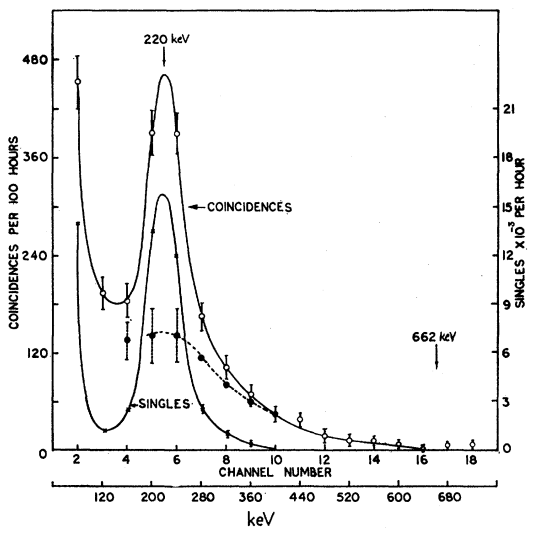


FIG. 6. Singles and coincidence pulse-height spectra due to the $\gamma$ rays scattered at 124° taken with 93.3-mg/cm²-thick lead. The dashed curve, obtained by subtracting the peak due to the secondary effects from the coincidence spectrum, represents the pulse-height spectrum due to the $\gamma$ rays scattered by the $K$-shell electrons.

[14] D. Strominger, J. M. Hollander, and G. T. Seaborg, Revs. Modern Phys. **30**, 585 (1958).

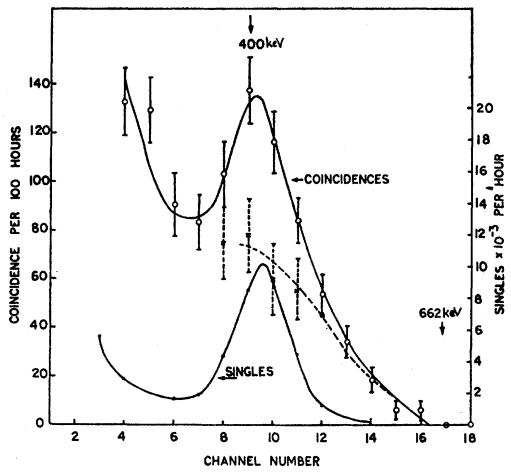


FIG. 7. Singles and coincidence pulse-height spectra due to the $\gamma$ rays scattered at 60° to the beam, taken with the 58.8-mg/cm²-thick lead scatterer. The dashed curve represents the pulse-height spectrum due to the $\gamma$ rays scattered by the $K$-shell electrons.

at various energies. Curve B of Fig. 8 shows this reconstructed spectrum, the area of which represents the intensity of the $\gamma$ rays scattered by the $K$-shell electrons in the lead scatterer. The intensity of the $\gamma$ rays scattered by the electrons in the Al scatterer is obtained from the area of the photopeak in the spectrum of Fig. 3 (shown by the crosses), and correcting it for the absorption of the 220-keV $\gamma$ rays in the NaI(Tl) crystal and its photopeak production efficiency. The number of electrons in the lead and the aluminum scatterer, respectively, is taken into account for the calculation of the scattering cross section. On the basis of the observed photon spectrum, above 160 keV, as shown in curve B of Fig. 8, the inelastic scattering cross section for scattered photons of energy greater than 160 keV at 124° is calculated to be

$$\sigma_K(124°)_{h\nu_2>160\,\mathrm{keV}}=(1.78\pm0.16)\sigma_F(124°),$$

where $\sigma_F$ is the cross section for a free electron. The error in the cross section is due to counting statistics. If the photon spectrum is extrapolated so as to have zero intensity at zero energy, the inelastic scattering cross section is estimated as $(2.14\pm0.20)\sigma_F(124°)$. On the other hand, if the photon spectrum is extrapolated as in Fig. 8, the value of the cross section is found to be $(2.35\pm0.21)\sigma_F(124°)$. There is no theoretical or experimental basis for the assumption of the photon spectrum at low energy as has been done above. At the same time, there is no physical reason to believe that the shape of the spectrum at the low-energy end would be drastically different from the above extrapolations. At the scattering angle of 60°—as is clear from Fig. 7—the low-energy part of the coincidence spectrum is very uncertain. No effort, therefore, has been made to calculate the inelastic scattering cross section at this angle.

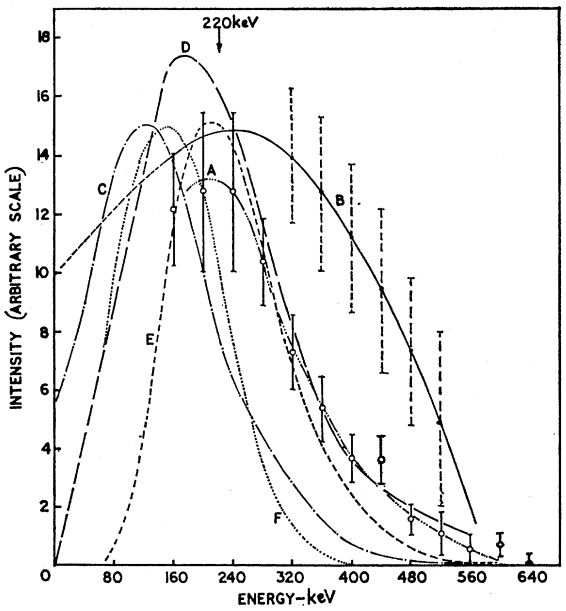


FIG. 8. Theoretically calculated and experimentally observed energy spectrum of the $\gamma$ rays scattered at 124° to the beam by the $K$-shell electrons of lead. Curve A (—···—···): experimentally observed pulse-height spectrum. Curve B (——): energy spectrum of the $\gamma$ rays obtained from experimentally observed pulse-height spectrum $A$. Curve C (—·—·): spectrum calculated from Bloch's theory. Curve D (— — —): Schnaidt's theory. Curve E (– – – – –): a classical treatment taking the $\beta^2$ term into account but neglecting the binding energy of the electron. Curve F (. . . . . .): Classical treatment taking the binding energy of the electron into account. The energy of the $\gamma$ rays scattered by a free electron at this angle is 220 keV.

## DISCUSSION

In Fig. 8 curve A represents the pulse-height spectrum, due to the scattered gamma rays, in the NaI(Tl) spectrum—as obtained from Fig. 6. Curve B was reconstructed, as mentioned earlier, from curve A to give the energy spectrum of the scattered photons. No correction has been applied for the energy resolution of the detector which only affects the high-energy end of the spectrum. It is clear that the energy of the $\gamma$ rays scattered from the $K$-shell electrons of lead at 124° extends from zero energy to about the maximum available energy of 570 keV. There are no theoretical calculations at the relativistic energies involved here, with which the observed results can be compared. The binding energy of the $K$-shell electron in lead is 88 keV. The momentum distribution for the electron as obtained from the relation of Podolsky and Pauling[15] for a hydrogen-like atom is given by $W(P)dP$, where

$$W_{K\text{ shell}}(P)dP=\text{const}\frac{P^2}{(P^2+0.358)^4}dP. \quad (1)$$

$P$ is in units of $m_0c$, $P=\beta/(1-\beta^2)^{\frac{1}{2}}$, and $\beta=v/c$. It is clear from Eq. (1) that momenta as high as 1 ($\beta=0.707$) are involved to a fair extent in the process.

Bloch[7] has calculated the energy spectrum of the $\gamma$ rays (energy $h\nu_1$) from the $K$-shell electron of an atom (binding energy $B$) for a case where (a) $h\nu_1 \ll m_0c^2$; (b) $B \ll W_e$, the energy transferred to the electron in the process; and (c) $\beta^2 \ll 1$. Evidently, none of the assumptions of the Bloch's theory hold in the present case. Also Bloch's theory gives the cross section to be the same as for a free electron, whereas the observed cross section is about double that. From this, it is clear that one cannot expect Bloch's theory to give the correct shape of the spectrum. Curve C of Fig. 8 is the scattered photon spectrum given by this theory and, as expected, does not fit the observed spectrum. Curve D in the figure is the spectrum given by the calculations of Schnaidt,[16] based on similar assumptions.

The energy spectrum of the scattered $\gamma$ rays can be calculated by applying the conservation of energy and momentum relations as was done by DuMond[2] in the case of x rays. In these calculations the electrons are assumed to be free but having a momentum distribution as given by Eq. (1). It is further assumed that the spectrum is cut off when the energy transferred to the electron becomes less than its binding energy in the atom. The conservation relations in this case are put as:

$$h\nu_1+m_0c^2/(1-\beta_1^2)^{1/2}=h\nu_2+m_0c^2/(1-\beta_2^2)^{1/2}, \quad (2)$$

and

$$(h\nu_1/c)+[m_0\beta_1c/(1-\beta_1^2)^{1/2}]a_1=(h\nu_2/c)p+[m_0\beta_2c/(1-\beta_2^2)^{1/2}]a_2, \quad (3a)$$

$$[m_0\beta_1c/(1-\beta_1^2)^{1/2}]b_1=(h\nu_2/c)q+[m_0\beta_2c/(1-\beta_2^2)^{1/2}]b_2, \quad (3b)$$

$$[m_0\beta_1c/(1-\beta_1^2)^{1/2}]c_1=(h\nu_2/c)r+[m_0\beta_2c/(1-\beta_2^2)^{1/2}]c_2, \quad (3c)$$

where $\beta_1c$ and $\beta_2c$ are the velocities of the electron before and after the scattering process; $a_1$, $b_1$, $c_1$ and $a_2$, $b_2$, $c_2$ are their direction cosines, respectively, taking the incident photon direction as the $x$ axis; $h\nu_1$ ($=hc/\lambda_1$) and $h\nu_2$ ($=hc/\lambda_2$) are the energies of the incident and the scattered photon, and $p$, $q$, $r$ are the direction cosines of the scattered photon. A solution of the above equation gives the wavelength $\lambda_2$ of the scattered photon as:

$$\lambda_2=\lambda_c+\frac{2\beta_1\lambda^*\cos\psi-(\lambda_c-\lambda_1)[1-(1-\beta_1^2)^{1/2}]}{1-\beta_1\cos\theta_1}. \quad (4)$$

In Eq. (4) the quantities $\lambda^*$, $\lambda_c$, $\psi$, and $\theta_1$ are the same

[15] B. Podolsky and L. Pauling, Phys. Rev. **34**, 109 (1929).

[16] F. Schnaidt, Ann. Physik **21**, 89 (1934).

as defined by DuMond[2]:

$$\lambda_c=\lambda_1+\frac{h}{m_0c}(1-\cos\theta), \tag{5a}$$

$$2\lambda^*=(\lambda_c^2+\lambda_1^2-2\lambda_c\lambda_1\cos\theta)^{1/2}. \tag{5b}$$

$\theta$ is the angle of scattering, $\psi$ is the angle between the initial electron momentum and the direction of momentum transfer in the case of normal Compton scattering, and $\theta_1$ is the angle between the directions of initial electron momentum and the incident photon. For a particular value of $\psi$ the angle $\theta_1$ can have values between $\psi+\phi$ and $\psi-\phi$, where $\phi$ is the angle between the direction of the incident photon and that of the Compton recoil electron initially at rest. When the angle of scattering $\theta=124°$ the angle $\phi=13°$ and the term $\cos\theta_1$ in Eq. (4) can be replaced by $\cos\psi$ without much error. Using the electron momentum distribution as given by Eq. (1), a treatment similar to that of DuMond[2] gives on graphical computation the spectrum of the scattered photons as given by curve E of Fig. 8.

The energy conservation relation of Eq. (2) is not strictly correct in the sense that the potential energy of the electron is not taken into consideration. As the sum of the potential and the kinetic energy of the electron in the orbit is constant and equal to its binding energy ($B=88$ keV for a lead $K$ electron), Eq. (2) should be modified as follows:

$$h\nu_1+m_0c^2-B=h\nu_2+m_0c^2/(1-\beta_2^2)^{1/2}, \tag{6}$$

whereas the momentum relations remain unchanged.

The scattered photon wavelength is then given by:

$$\lambda_2=\lambda_c+\frac{2\lambda^*P\cos\psi+P^2\lambda_c/2\alpha+\lambda_c(1-A)-\lambda_1B/m_0c^2}{A-P\cos\theta_1-P^2/2\alpha}, \tag{7}$$

where

$$A=1-(B/m_0c^2)-(B/2h\nu_1)(2-B/m_0c^2)$$

and

$$\alpha=h\nu_1/m_0c^2.$$

All other symbols are as defined earlier in the text. The scattered photon spectrum calculated from this relation in a way similar to that from Eq. (4) is shown by Curve F of Fig. 8. In computing the photon spectrum from Eq. (7), as also from Eq. (4), the cross section of the scattering process is presumed to be independent of the initial electron momentum.

It should be mentioned that both the relations (4) and (7) suffer from the defect that the possible momentum transfer to the atom, during the time the electron is going out of its Coulomb field, is not taken into consideration. This effect is expected to contribute more to the higher energy region of the scattered gamma-ray spectrum. It is evident from Fig. 8 that the spectra calculated from the various theories differ to a very great extent from the observed gamma-ray spectrum. It points to the necessity of a rigorous theoretical treatment of the process of incoherent gamma-ray scattering by tightly bound electrons at relativistic energies.

## ACKNOWLEDGMENTS

The authors acknowledge the tremendous help rendered by N. L. Ragoowansi and P. J. Bhalerao in constructing and maintaining all the electronics used in the experiment, as also in the numerical computations. We are thankful to Dr. B. Saraf for many helpful discussions, and to Dr. F. Bloch and Dr. Jesse W. M. DuMond for their comments.